

Determination of the energy-spectrum parameters of semimetallic $\text{Hg}_{1-x}\text{Cd}_x\text{Te}$ by the method of tunnel spectroscopy in a magnetic field

L. P. Zverev, V. V. Kruzhaev, G. M. Min'kov, and O. É. Rut

A. M. Gorkii Ural State University

(Submitted 10 July 1980)

Zh. Eksp. Teor. Fiz. **80**, 1163–1173 (March 1981)

An investigation of the oscillations of tunnel conductivity of the structures $\text{Hg}_{1-x}\text{Cd}_x\text{Te}-\text{Al}_2\text{O}_3-\text{Pb}$ ($0 \leq x \leq 0.16$) in a magnetic field at various junction voltages makes it possible to determine in experiment the dispersion law and the dependence of the effective carrier mass and of the g factor on energy. For a sample with $x = 0.16$, a linear dependence of the energy on the quasimomentum was observed. The results are well described within the framework of Kane's three-band approximation. The parameters P , ϵ_g , m_n , ϵ_F and the g factor of the investigated samples were determined. The possible uses of the method are discussed.

PACS numbers: 73.40.Rw

The method of tunnel spectroscopy is at present used to study the energy spectra of semiconductors and semimetals. The investigation of tunnel conductivity in metal-insulator-semiconductor structures yields as a rule information only on the characteristic energies of the electron spectrum and of the spectra of the elementary excitations, whereas the dispersion law and the state density cannot be obtained without significant assumptions concerning the shape of the potential barrier and the dependence of the tunneling probability on the energy and quasimomentum, which are not sufficiently well known under the experimental conditions. The capabilities of tunnel spectroscopy become greatly expanded when the investigations are performed in quantizing magnetic fields. In this case singularities connected with the Landau levels are produced in the state density of the investigated material, and this leads to oscillations of the tunnel conductivity as a function of the magnetic field and of the applied voltage. This was demonstrated in the study of the spectrum of two-dimensional surface electrons in n -InAs and n -PbTe.^{2,3} The method makes it also possible to investigate the spectrum of the carriers in the volume. Thus, the dispersion law was measured in experiment⁴ and the energy dependence of the effective mass of the volume electrons of n -InAs was obtained.⁵

Investigations of gapless semiconductors (HgTe, HgSe, $\text{Hg}_{1-x}\text{Cd}_x\text{Te}$) by the method of tunnel spectroscopy in the absence of a magnetic field were performed in Refs. 6 and 7, where the energies of the optical phonons in these materials were determined. An attempt was made in Ref. 8 to investigate the tunnel conductivity of the structures $\text{HgTe}(\text{HgSe})-\text{Al}_2\text{O}_3-\text{Pb}$ in a magnetic field, but it appears that the poor quality of the junctions did not make it possible to obtain reliable results.

The possibility of obtaining extensive information on the energy spectrum makes it urgent to study further gapless semiconductors by the method of tunnel spectroscopy in a magnetic field. This method is particularly convenient for the study of the spectra of solid solutions (such as $\text{Hg}_{1-x}\text{Cd}_x\text{Te}$), for which it is technologically difficult to obtain a set of samples of the same

composition with different carrier densities, a necessary condition for the use of traditional methods.

1. SAMPLE PARAMETERS. PREPARATION OF TUNNEL JUNCTIONS

We report here the experimental results of an investigation of the tunnel conductivity of $\text{Hg}_{1-x}\text{Cd}_x\text{Te}-\text{Al}_2\text{O}_3-\text{Pb}$ structures in a magnetic field up to 60 kOe at 4.2 K. To determine the parameters of the investigated samples we measured the dependences of the Hall constant (R) on the magnetic field at 4.2, 77, and 300 K, as well as the magnetoresistance at 4.2 K. Typical $R(H)$ plots are shown in Fig. 1. For samples 1, 2, and 3 (see Table I) the Hall constant is independent of the magnetic field, thus pointing to the presence of one type of carrier. In this case R determines the density and the sign of the carriers, which are holes in samples 1 and 3 and electrons in sample 2. The absence in samples 1 and 3 of an electron contribution to the Hall effect in weak magnetic fields, and the presence in sample 2 of Shubnikov-de Haas oscillations, whose period yields a concentration close to the Hall value, are evidence that the carriers in these samples belong to the bands and consequently the Fermi level lies in

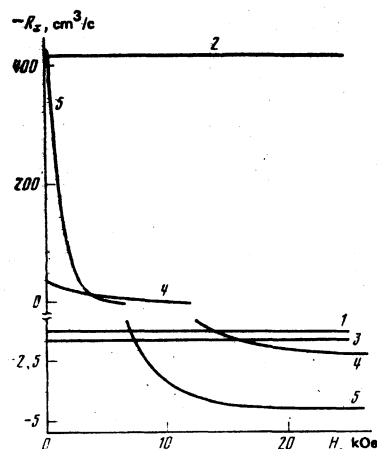


FIG. 1. Typical plots of R against the magnetic field. $T = 4.2$ K. The numbers on the curves correspond to the numbers of the samples in Table I.

TABLE I. Parameters of investigated $\text{Hg}_{1-x}\text{Cd}_x\text{Te}$ samples.

Sample No.	x	R_{oc} , cm^2/c	n, p , cm^{-3}	$P \cdot 10^4$, $\text{eV} \cdot \text{cm}$	ϵ_g , meV	m_n/m_0	ϵ_F , meV
1	0	+1.23	$5.1 \cdot 10^{18}$	7.8 ± 0.2	-300 ± 15	0.0272	-8 ± 2
2	0	-416	$1.5 \cdot 10^{18}$	—	—	—	7 ± 2
3	0.05 ± 0.01	+1.60	$3.9 \cdot 10^{18}$	8.6 ± 0.2	-245 ± 15	0.0184	-6 ± 2
4	0.11 ± 0.01	+2.30	$2.7 \cdot 10^{18}$	8.7 ± 0.2	-110 ± 15	0.0082	6 ± 2
5	0.16 ± 0.01	+4.50	$1.4 \cdot 10^{18}$	8.5 ± 0.2	0 ± 5	≈ 0	10 ± 2

the valence or in the conduction band.

In samples 4 and 5, the Hall constant is negative in weak fields and reverses sign with increasing magnetic field. This behavior is typical of the case when the conductivity is due to two types of carrier, with opposite signs, and indicates that the Fermi level lies in the conduction band. The dependence is qualitatively analogous for different pairs of Hall junctions, but the quantitative characteristics (R as $H \rightarrow 0$ and the field at which the Hall constant reverses sign) are different. The cited measurements can therefore be used to determine only the Hall density from the value of the Hall constant in a strong magnetic field, which for samples 4 and 5 amounts to $p = (1-2) \times 10^{18} \text{ cm}^{-3}$. Thus, for samples 1 and 3-5 the Hall density at 4.2 K exceeds 10^{18} cm^{-3} and therefore the intrinsic carrier density cannot be determined from the value of the Hall constant at room temperature.⁹ An attempt to determine the composition from the value of R at $T = 300 \text{ K}$ can lead to a substantial error (up to 0.04) in the value of x . The compositions of the investigated samples (see Table I) was determined by us by an x-ray microanalysis.

The tunnel junctions were made from single-crystal samples cut into parallelepipeds with dimensions $\approx 6 \times 3 \times 1 \text{ mm}$. After mechanical grinding and polishing, the samples were etched in 10% solution of bromine in methanol. A layer of aluminum 30-50 Å thick was sputtered on the freshly etched surface in a vacuum of 10^{-6} Torr . After complete oxidation of the aluminum, the sample surface was insulated with collodion, with the exception of a strip in the middle 0.3-0.5 mm wide, across which metallic electrodes (lead strips) were sputtered in a vacuum of 10^{-6} Torr through a mask. The ohmic contacts were soldered with indium. The tunnel junctions had an area $(1-2) \times 10^{-3} \text{ cm}^2$ and a resistance from 10 to 1000 Ω, which varied little in the temperature interval 4.2-300 K.

Measurements of the differential resistance $\partial V/\partial I$ and of its derivative $\partial^2 V/\partial I^2$ were made by a four-probe method. Evidence that the current at 4.2 K is of tunneling origin was the characteristic singularity of the conductivity at low bias, due to the superconductivity of the lead, which was made to vanish in a magnetic field $\approx 1 \text{ kOe}$. On the whole, the current-voltage characteristic was similar to those given in Ref. 6-8.

The measurements were made on two or three tunnel junctions for each sample.

2. EXPERIMENTAL RESULTS

The main measurements were made at a magnetic-field orientation $\mathbf{H} \perp \mathbf{I}$ (the magnetic field was parallel to the plane of the tunnel junction), so as to exclude the possible contribution of two-dimensional states that

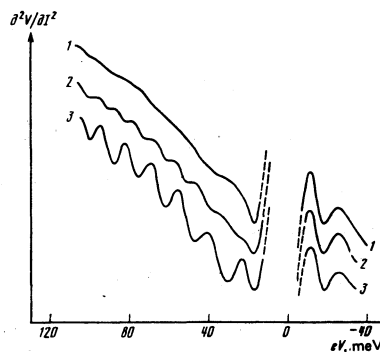


FIG. 2. Dependence of $\partial^2 V/\partial I^2$ on the voltage across the tunnel junction for sample 1. Magnetic field, kOe: 1) 1.3, 2) 31.2, 3) 41.2.

can exist on the surface of the semiconductor or in the barrier, as they are not quantized in this orientation.¹⁰

In all the investigated samples, in fields starting with 6-20 kOe (for different samples), oscillations connected with the Landau levels were observed in the dependence of the tunnel conductivity on the applied voltage and on the magnetic field (Figs. 2 and 3). At a fixed voltage (Fig. 3) the oscillations are periodic in the reciprocal field, with a period that depends on the applied voltage. This is clearly seen in Fig. 4, where the position of the maxima of $\partial^2 V/\partial I^2 = \partial^2 V/\partial I^2(H)$ with respect to the reciprocal magnetic field is plotted as a function of the number of the oscillations.

Figure 5 shows the position of the maxima of $\partial^2 V/\partial I^2$ against the magnetic field. These dependences do not yield directly the position of the Landau levels, for two reasons. First, the minimum of the differential resistance (the maximum of the tunnel conductance) can be shifted relative to the junction voltage at which the Landau level and the state density of the semiconductor cross an energy corresponding to the Fermi energy of the metal. The reason for this shift is the dependence of the tunneling probability on the energy and on the quasimomentum.¹¹ This can lead to a change in the phase of the observed oscillations. Second, Fig. 5 shows the position of the maxima of $\partial^2 V/\partial I^2$ are not of $\partial I/\partial V$, and this yields an additional phase shift by $\pi/2$. In the case when the total phase shift does not depend on the magnetic field and on the applied voltage (as will be shown below, this is satisfied for the samples

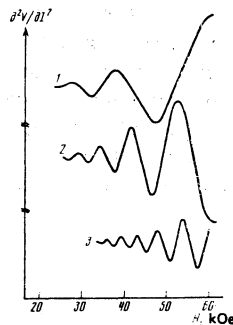


FIG. 3. Dependence of $\partial^2 V/\partial I^2$ on the magnetic field for sample 1. Junction voltage, mV: 1) +50, 2) +80, 3) +140. The sign of the voltage corresponds to the sign of the potential on the $\text{Hg}_{1-x}\text{Cd}_x\text{Te}$.

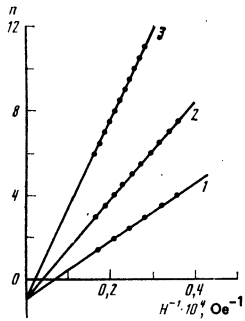


FIG. 4. The position of the oscillations in terms of the reciprocal magnetic field vs. the number of the oscillations for sample 1. Junction voltage, mV: 1) +60, 2) +90, 3) +140.

investigated by us), the period of the oscillations in terms of the reciprocal magnetic field at a bias V , in the case of an isotropic dispersion law, determines the quasimomentum at the energy $\varepsilon = \varepsilon_F + eV$ (Ref. 4):

$$k_{x, y, z}^2 = \frac{2e}{c\hbar\Delta(1/H)_v} \quad (1)$$

The dependences of k^2 on eV obtained in this manner for the investigated samples are shown in Fig. 6. It is seen that for all the samples the dispersion laws are essentially nonparabolic. With increasing x , the slope of the plot of $eV(k^2)$ at small values of the quasimomentum increases, corresponding to a decrease of the effective mass at the bottom of the band.

Using the results shown in Fig. 5 we can determine the dependence of the cyclotron mass on the energy (or quasimomentum) with the aid of the relation

$$m_e(\varepsilon) = \frac{\hbar e H}{c e (V_{n+1} - V_n)} \quad (2)$$

This expression determines the effective mass at the energy $\varepsilon = \varepsilon_F + e(V_{n+1} + V_n)/2$ or at the quasimomentum corresponding to this energy [see Eq. (1)]. The experimental dependences of the electron mass on the quasimomentum are shown in Fig. 7.

3. COMPARISON WITH THEORY AND DISCUSSION

It is known that the ternary compounds $\text{Hg}_{1-x}\text{Cd}_x\text{Te}$ with $x < 0.16$ have an inverted band structure, wherein the conduction band is Γ_6 , degenerate at $k=0$ with the heavy-hole band. In Kane's three-band model, the

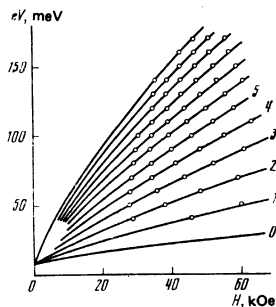


FIG. 5. Dependence of the positions of the maxima of $\partial^2 V / \partial I^2$ on the magnetic field for sample 1. Solid lines—calculated from expression (4). The numbers at the curves correspond to the numbers of the Landau levels.

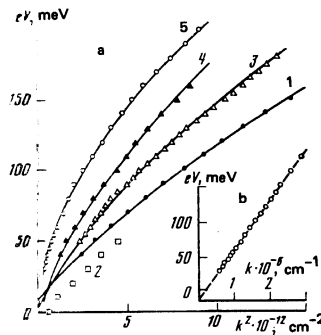


FIG. 6. Dispersion laws of investigated samples. Points—experimental results. The numbers 1–5 correspond to the numbers of the samples in Table I. Solid curves—theoretical plots with the parameters listed in the table. Figure 6b illustrates the linear dispersion law for sample 5.

energy spectrum of such a semiconductor is described by the solutions of the equation¹²

$$(e' - \varepsilon_e) e' (e' + \Delta) - k^2 P^2 (e' + 2\Delta/3) = 0, \quad (3)$$

where $e' = \varepsilon - \hbar^2 k^2 / 2m_0$, P is the matrix element of the momentum operator, $\varepsilon_g = \varepsilon(\Gamma_6) - \varepsilon(\Gamma_8)$, $\Delta = \varepsilon(\Gamma_8) - \varepsilon(\Gamma_7)$, and the energy is reckoned from the points of degeneracy of the bands Γ_8 . Replacing in (3) k^2 by $2eH(n+1/2)/c\hbar$,¹³ we can obtain an equation that describes the motion of the quasiclassical Landau levels in a magnetic field. Expanding this expression in powers of $(\varepsilon - e')/\varepsilon$ and neglecting in $\partial(k^2)/\partial\varepsilon$ terms of order of ε/Δ , we have

$$H_n(\varepsilon) = c\hbar \varepsilon (\varepsilon - \varepsilon_e) (\varepsilon + \Delta) / 2e(n+1/2) (\varepsilon + 2\Delta/3) \left[P^2 + \frac{3\hbar^2}{2m_0} (\varepsilon - \varepsilon_g/2) \right]. \quad (4)$$

Equation (4) does not include the spin splitting, inasmuch as no splitting of the Landau levels is observed in the tunnel conductivity at $H \perp I$.

In the approximation $\varepsilon \ll 2\Delta/3$ we can obtain simple analytic expressions for the dispersion law and for the dependence of the effective mass on the quasimomentum:

$$\varepsilon(k) = \frac{\hbar^2 k^2}{2m_0} + \frac{\varepsilon_g}{2} \left[1 - \left(1 + \frac{8k^2 P^2}{3\varepsilon_g^2} \right)^{1/2} \right], \quad (5)$$

$$m_e(k) = \left(\frac{1}{\hbar^2 k} \frac{\partial \varepsilon}{\partial k} \right)^{-1} = \left[\frac{1}{m_0} - \frac{4P^2}{3\hbar^2 \varepsilon_g} \left(1 + \frac{8k^2 P^2}{3\varepsilon_g^2} \right)^{-1/2} \right]^{-1}. \quad (6)$$

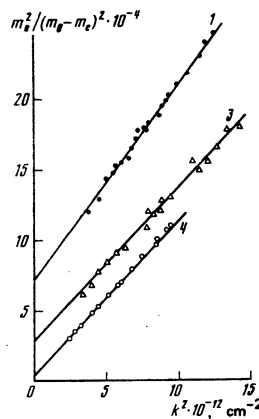


FIG. 7. Plot of $m_e^2 / (m_0 - m_e)^2$ vs. k^2 . The numbers 1, 3, and 4 correspond to the numbers of the samples in Table I.

At $k=0$ expression (6) yields the connection between P , ε_g , and the mass m_n at the bottom of the band:

$$P^2 = \frac{3\varepsilon_g \hbar^2}{4} \left(\frac{1}{m_0} - \frac{1}{m_n} \right). \quad (7)$$

Rewriting (6) in the form convenient for comparison with experiment, we obtain

$$\left(\frac{m_n(k)/m_0}{1 - m_n(k)/m_0} \right)^2 = \frac{9\varepsilon_g^2 \hbar^4}{16P^2 m_0^2} + \frac{3\hbar^4}{2P^2 m_0^2} k^2 = \left(\frac{m_n/m_0}{1 - m_n/m_0} \right)^2 + \frac{3\hbar^4}{2P^2 m_0^2} k^2. \quad (8)$$

Thus, the dependence of $m_n^2(k)/(m_0 - m_n(k))^2$ on k^2 should be linear, and the slope and the point of extrapolation to $k=0$ make it possible to determine P , m_n , and also, using (7), the value of ε_g .

Plots of $m_n^2(k)/(m_0 - m_n(k))^2$ against k^2 are shown in Fig. 7. It is seen that the experimental points lie well on a straight line, and the mass at the bottom of the band decreases with increasing x . The experimentally determined parameters of the dispersion law for the investigated samples are given in Table I. Using these parameters, we can plot the dispersion laws (5) and, by making an energy shift, (i.e., by choosing ε_F) fit them to the experimental plots of eV against k^2 (Fig. 6a). The Fermi energy values chosen in this manner (see Table I) agree qualitatively with the Hall-measurement data.

The set of parameters determined by us for HgTe (sample 1) agrees satisfactorily with the published parameters.⁴ This, as well as the qualitative agreement with the results of Hall measurements is evidence that the tunnel-conductivity oscillations observed by us are due to quantization of the volume-carrier spectrum. This is already indicated by the results of measurements made on n -HgTe (sample 2), obtained by isothermal annealing of sample 1 in mercury vapor at $T = 300^\circ\text{C}$ for 120 hours. The period of the Shubnikov-de Haas oscillations in this sample agree with the period of the tunnel-conductivity oscillations at zero bias. We were unable to determine the set of band parameters and compare it with the results obtained by us for p -HgTe, inasmuch as the oscillations had a small amplitude and were observed in a narrow bias range. Figure 8 shows the values of the width of the forbidden band and of m_n for samples with different compositions. It is seen that the experimental results are in fair agreement with the known relations.¹⁴

Of particular interest is sample 5, in which m_n and ε_g are close to zero. In this case, starting with suf-

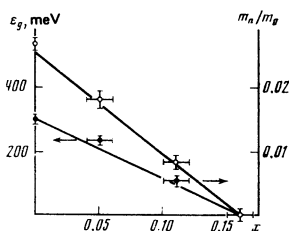


FIG. 8. Dependences of the width of the forbidden band and of the effective mass of the electrons at the bottom of the band on the composition in the case of $\text{Hg}_{1-x}\text{Cd}_x\text{Te}$. Points—present results, solid lines—results of Ref. 14.

ficiently small k , the condition $8k^2P^2/3\varepsilon_g^2 \gg 1$ is satisfied (thus, e.g., at $|\varepsilon_g| = 0.02$ eV we have $8k^2P^2/3\varepsilon_g^2 \approx 40$ already at $k = 1 \times 10^6 \text{ cm}^{-1}$). Recognizing that $m_0 \gg m_n$, the dispersion law (5) for these quasimomenta can be written in the form

$$\varepsilon = \varepsilon_F + eV = \varepsilon_g/2 + (2/3)^{1/2} kP, \quad (9)$$

i.e., the $\varepsilon = \varepsilon(k)$ dependence should be linear. Our experimental results (Fig. 6b) show that the dispersion law for sample 5 is indeed close to linear. From the slope $\tan \alpha = (2/3)^{1/2} P$ we can determine P , and the point of extrapolation to $k=0$ in Fig. 6b yields $\varepsilon_g/2 - \varepsilon_F$. Reducing the results in this manner we obtain a value of P which agrees with that determined from the dependence of the mass on the quasimomentum. The value $\varepsilon_g/2 - \varepsilon_F = 10$ meV also indicates that the width of the forbidden band in this sample is close to zero.

The parameters of the spectrum (ε_g , P , m_n) can also be obtained by describing the dependence of the position of the maxima of $\partial^2 V / \partial I^2$ on the magnetic field (Fig. 5) by Eq. (4), in which $n + 1/2$ must be replaced by $n + \varphi$. The causes of the need for introducing an additional phase shift were discussed in Sec. 2 above. Recognizing that $\varepsilon = \varepsilon_F + eV$, we see that by minimizing the mean squared deviation of the experimental points from the theoretical curves we can obtain all four parameters P , ε_g , ε_F , and φ . Such a reduction of the experimental results is justified if φ does not depend on the magnetic field and on the junction voltage. Satisfaction of this condition can be verified by means of the dependence of the number of the oscillations on the reciprocal magnetic field. In fact, writing (4) in the form

$$n = \frac{c\hbar}{2eH_n} \frac{e(\varepsilon - \varepsilon_g)(\varepsilon + \Delta)}{(\varepsilon^2 + \Delta^2) [P^2 + (3\hbar^2/2m_0)(\varepsilon - 1/2\varepsilon_g)]} - \varphi, \quad (10)$$

we find that if φ is constant, then the dependence of n on $1/H$ should be linear and should be extrapolated as $1/H \rightarrow 0$ to a single point ($n = -\varphi$) for all the values of the bias. For the samples investigated by us, the condition that φ be constant is satisfied (Fig. 4). The values of P , ε_g , m_n , and ε_F obtained by computer minimization agree within the accuracy limits with those given in Table I. Figure 5, which shows the theoretical $eV_n(H)$ curves with the parameters determined by us shows good agreement with the experimental results.

4. SPIN SPLITTING

In addition to the investigation of the tunnel-conductivity oscillations at a magnetic-field orientation $\mathbf{H} \perp \mathbf{I}$, measurements were made at $\mathbf{H} \parallel \mathbf{I}$. In this case, oscillations similar to those described above are observed in samples 1 and 3, except that they are shifted in phase. The values of P , ε_g , m_n , and ε_F determined at $\mathbf{H} \parallel \mathbf{I}$ agree with those listed in Table I. In samples 4 and 5 with small effective mass, a splitting of the tunnel-conductivity oscillations is observed (Figs. 9 and 10). It is seen from the figures that this splitting at small values of the bias leads practically to a doubling of the oscillation frequency (compared with the $\mathbf{H} \perp \mathbf{I}$ orientation) and decreases with increasing eV. For large bias, when the splitting cannot be observed, the period of the oscillations is the same in both mag-

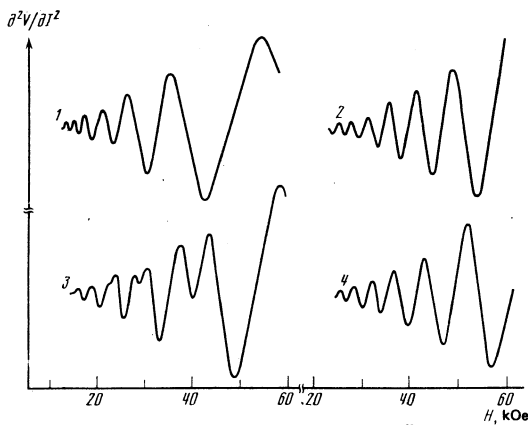


FIG. 9. Oscillations of the tunnel conductivity for two orientations of the magnetic field [1, 2) $H \perp I$, 3, 4) $H \parallel I$]. Junction voltage, mV: 1, 3) +110, 2, 4) +180. Sample 5.

netic-field orientations.

It is most natural, in our opinion, to relate the observed singularities with the spin splitting of the Landau levels. In this case we can determine from the splitting Δ (eV) the electron g -factor:

$$g = \Delta(eV) / \mu_B H, \quad (11)$$

where μ_B is the Bohr magneton. The experimental values of the g factor is a function of the energy are shown in Fig. 11. The figure shows also the theoretical curves in Kane's three-band model¹⁵

$$g(\epsilon) = 2 \left[1 - \left(\frac{m_0}{m_e(\epsilon)} - 1 \right) \frac{\Delta}{2\Delta + 3\epsilon} \right], \quad (12)$$

calculated using the experimental values of $m_e(\epsilon)$.

The theoretical dependences agree well with the experimental results. It remains unclear why the splitting is observed only at a magnetic-field orientation $H \parallel I$ and not at $H \perp I$. Unfortunately, we do not know of any theoretical studies in which spin is taken into account in the analysis of tunneling in a magnetic field.

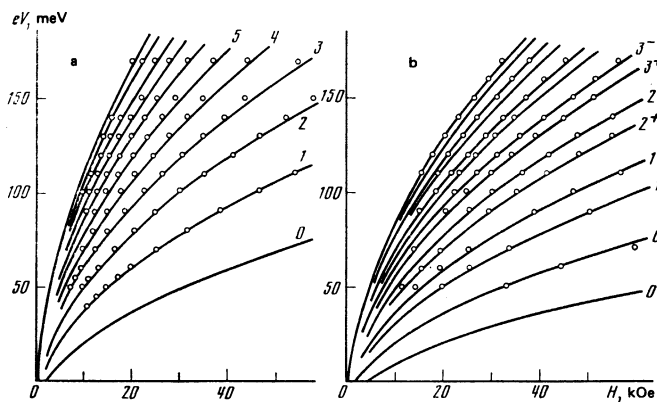


FIG. 10. Positions of the maxima of $\partial^2 V / \partial I^2$ vs. the magnetic field and the junction voltage for sample 5; a) $H \perp I$, b) $H \parallel I$. Solid curve—calculation from Kane's three-band model. The numbers on the curves correspond to the numbers of the Landau levels (the superscripts + and - pertain to the spin-split levels).

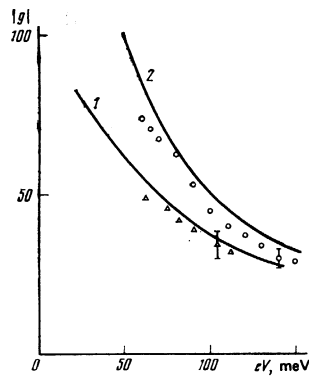


FIG. 11. Dependence of the g factor on the energy: \circ) sample 4, Δ) sample 5. 1 and 2) theoretical plots calculated from expression (12).

5. CONCLUSION

We have investigated the tunnel conductivity of $Hg_{1-x}Cd_xTe-Al_2O_3-Pb$ junctions at 4.2 K in a magnetic field. Oscillations due to the quantization of the spectrum of the volume carriers were observed. The dispersion law and the energy dependences of the effective mass and of the g factor were determined for the investigated samples. The results are well described within the framework of Kane's three-band approximation; this made it possible to determine the energy-spectrum parameters P , ϵ_g , m_n , and ϵ_F . In the approximation used in the paper, no account was taken of the influence of the remote bands, whose contribution must be taken into consideration in a number of cases when the experimental results are reduced. Thus, it was shown in Ref. 13 that allowance for the influence for the remote bands in HgSe changes quite substantially (by up to 50%) the value of the g -factor and has a negligible influence on the effective mass. Since the relative contribution of the remote bands decreases with decreasing width of the forbidden band, and the spin splitting was observed only for materials with $|\epsilon_g| \leq 110$ meV, this contribution should be negligible, thus justifying the use of the three-band model. In addition, the scatter of the γ parameters cited in the literature is large enough, so that an attempt to take into account the contribution of the remote bands in the reduction of the presented experimental results seems inadvisable to us.

It should be noted that usually the results of investigations of galvanomagnetic effects in $p-Hg_{1-x}Cd_xTe$ ($N_A > N_D$) are interpreted with account taken of the resonant acceptor states, which produce a maximum of the state density against the backgrounds of the continuous spectrum of the conduction band. No such state-density singularity appears in our results on tunnel spectroscopy. The reason, in our opinion, is that even in samples 4 and 5, in which an electronic contribution to the Hall effect was observed in weak magnetic fields, the acceptor density is so high ($N_A > 10^{18} cm^{-3}$), that the acceptor band, even if it is not merged with the heavy-hole band, is greatly broadened and does not produce a substantial maximum in the state density. This is evidenced also by the small value ($\Delta\rho/\rho \approx 0.1-0.15$) of the longitudinal and transverse magnetoresistances in

these samples.

Thus, the results show that the method of tunnel spectroscopy in a magnetic field makes it possible to obtain directly in experiment the dispersion law and the energy dependence of the effective mass of a gapless semiconductor, without resorting to concrete models; such a procedure offers a number of advantages over the traditional galvanomagnetic and magneto-optical measurements.

The authors thank I. M. Tsidril'kovskii and the staff members of the Semiconductor Laboratory of the Institute of Metal Physics of the Ural Scientific Center of the USSR Academy of Sciences for supplying the samples and for a helpful discussion.

¹E. Wolf, Nonsuperconducting Electron Tunneling Spectroscopy, *Solid State Physics*, **30**, 1 (1975).

²D. C. Tsui, *Phys. Rev.* **B8**, 2657 (1973).

³D. C. Tsui, G. Kaminsky, and P. H. Schmidt, *Phys. Rev.* **B9**, 3524 (1974).

⁴L. P. Zverev, V. V. Kruzhaev, and G. M. Min'kov, *Pis'ma Zh. Eksp. Teor. Fiz.* **29**, 402 (1979) [*JETP Lett.* **29**, 365 (1979)].

⁵L. P. Zverev, V. V. Kruzhaev, G. M. Min'kov, and O. É. Rut, *ibid.* **31**, 169 (1980) [**31**, 154 (1980)].

⁶J. Niewodniczanska-Zawadzka and J. Rauluszkiewicz, *Phys. Stat. Sol. (b)* **74**, K93 (1976).

⁷J. Niewodniczanska-Zawadzka and J. Grembowicz, *ibid.* **91**, K13 (1979).

⁸J. Niewodniczanska-Zawadzka and J. Rauluszkiewicz, *Proc. 13th Int. Conf. on Semicond. Phys. Rome, 1976*, p. 433.

⁹R. V. Lutsiv, P. P. Petrov, N. A. Rud', M. V. Matviiv, and N. M. Sol'skii, *Izv. AN SSSR, neorgan. mater.* **12**, 830 (1976).

¹⁰D. C. Tsui, *Phys. Rev.* **B4**, 4438 (1971).

¹¹G. M. Min'kov and V. V. Kruzhaev, *Fiz. Tverd. Tela (Leningrad)* **22**, 1641 (1980) [*Sov. Phys. Solid State* **22**, 959 (1980)].

¹²I. M. Tsidil'kovskii, *Élektrony i dyrki v poluprovodnikakh (Electrons and Holes in Semiconductors)*, Nauka, 1972, Chap. 3.

¹³A. I. Pnomarev, G. A. Potapov, G. I. Kharus, and I. M. Tsidil'kovskii, *Fiz. Tekh. Poluprov.* **13**, 854 (1979) [*Sov. Phys. Semicond.* **13**, 502 (1979)].

¹⁴J. D. Willey and R. N. Dexter, *Phys. Rev.* **181**, 1181 (1969).

¹⁵P. Kacman and W. Zawadski, *Phys. Stat. Sol. (b)* **47**, 629 (1971).

Translated by J. G. Adashko